physica status solidi a
www.pss-a.com
applications and materials science

STM imaging of carbon nanotube point defects

Z. Osváth, L. Tapasztó, G. Vértesy, A. A. Koós, Z. E. Horváth, J. Gyulai, and **L. P. Biró**

Research Institute for Technical Physics and Materials Science, 1525 Budapest, P.O. Box 49, Hungary

Received 12 October 2006, revised 27 February 2007, accepted 27 February 2007
Published online 23 May 2007

PACS 61.46.Fg, 61.80.Jh, 68.37.Ef, 68.37.Ps, 81.07.De

In this work the STM investigation of nanotube point defects created by ion irradiation (e.g. vacancies) is presented. The defects appeared as hillock-like features on the STM images. These defects were compared with similar features observed on the STM images of as-grown coiled carbon nanotubes. In this case the observed hillock-like features were attributed to the non-hexagonal carbon rings, which are responsible for the growth of bent and coiled nanotube structures. For irradiation, multi-walled carbon nanotubes produced by the arc-discharge method were dispersed on highly oriented pyrolitic graphite (HOPG) surface and irradiated with Ar^+ ions of 30 keV, using a low dose of $D = 5 \times 10^{11}$ ions/cm^2.

phys. stat. sol. (a) **204**, No. 6, 1825–1829 (2007) / **DOI** 10.1002/pssa.200675330

Original Paper

phys. stat. sol. (a) **204**, No. 6, 1825–1829 (2007) / **DOI** 10.1002/pssa.200675330

STM imaging of carbon nanotube point defects

Z. Osváth*, **L. Tapasztó, G. Vértesy, A. A. Koós, Z. E. Horváth, J. Gyulai,** and **L. P. Biró**

Research Institute for Technical Physics and Materials Science, 1525 Budapest, P.O. Box 49, Hungary

Received 12 October 2006, revised 27 February 2007, accepted 27 February 2007
Published online 23 May 2007

PACS 61.46.Fg, 61.80.Jh, 68.37.Ef, 68.37.Ps, 81.07.De

In this work the STM investigation of nanotube point defects created by ion irradiation (e.g. vacancies) is presented. The defects appeared as hillock-like features on the STM images. These defects were compared with similar features observed on the STM images of as-grown coiled carbon nanotubes. In this case the observed hillock-like features were attributed to the non-hexagonal carbon rings, which are responsible for the growth of bent and coiled nanotube structures. For irradiation, multi-walled carbon nanotubes produced by the arc-discharge method were dispersed on highly oriented pyrolitic graphite (HOPG) surface and irradiated with Ar^+ ions of 30 keV, using a low dose of $D = 5 \times 10^{11}$ ions/cm^2.

1 Introduction

Carbon nanotubes (CNTs) may contain different kinds of topological point defects in their structure, like non-hexagonal carbon rings, or vacancy-related defects. These can play important role in the applications since their presence affect mechanical [1] and transport properties [2]. Topological point defects can form during the nanotube growth process or they can be introduced after synthesis for example by chemical purification [3] or irradiation by charged particles [4, 5]. If specific configurations of non-hexagonal carbon rings (e.g. pentagon-heptagon pairs) are incorporated into the nanotube structure during the growth process, bent nanotubes [6, 7], Y-branched nanotube junctions [8], or regularly coiled carbon nanotubes [9, 10] can form. The signatures of such defects were observed by UHV STM operated at low temperature during the investigation of a bent nanotube junction [11, 12] or at the end of a single wall nanotube [13]. The identification of the pentagon-heptagon pairs (in the case of bent junction), or single pentagon rings (in the case of nanotube end) was possible by comparing the experimental results with simulations.

Irradiation experiments with both electrons [4, 14] and heavy ions [5] show that irradiation modifies the structure and dimensions of CNTs. These structural changes can be explained by the mono and bi-vacancies created by electrons and ions [14, 15], which can transform into non-hexagonal carbon rings by dangling bond saturation [14, 16]. Carbon nanotube point defects induced by electron beam were successfully observed during high resolution TEM investigations [17]. The irradiation-induced effects in carbon nanotubes have been addressed recently in a brief overview by Krasheninnikov and co-workers [15].

The STM signatures of native topological CNT defects were also simulated [18, 19] and the STM image of individual vacancies in single wall CNTs were predicted [20]. Simulations showed that different type of vacancy-related defects have different shapes in the STM images [21]. In this work we present an experimental STM study of nanotube point defects created by ion irradiation of multi-wall CNTs.

* Corresponding author: e-mail: osvath@mfa.kfki.hu, Phone: +36 1 392 2222 ext. 1157, Fax: +36 1 392 2226

Furthermore, the signatures of topological defects were observed on as-grown coiled carbon nanotubes as well.

2 Experimental

In this experiment we used multi-wall CNTs grown by the arc discharge method. The details of the growth process were described elsewhere [22]. A suspension was prepared by sonicating 1 mg of CNT sample in 20 ml of toluene for 60 min. Droplets of this suspension were dispersed on a cleaved HOPG substrate. After the deposition of the CNTs the toluene was allowed to evaporate. The sample was introduced in an ion implanter and was irradiated with Ar^+ ions of 30 keV using a low dose of $D = 5 \times 10^{11}$ ions/cm^2. The ion current density was $J = 0.9$ nA/cm^2 and the irradiation was done at normal incidence. The low dose was used in order to create individual, non-overlapping defects in the nanotube walls. The irradiated sample was investigated by STM (constant current mode) in air. These measurements were done with a Nanoscope *E* instrument operating under ambient conditions, with tunneling currents (I_t) of 0.3–1 nA and bias voltages (U_t) in the range of 0.1–0.5 V. Complementary contact mode AFM measurements on the irradiated HOPG substrate were done with the same Nanoscope *E* instrument operating in constant force mode, in air. The contact force between the AFM tip and the sample was kept as low as possible (order of 10^{-9} N).

The coiled carbon nanotubes observed in this work were synthesized by the catalytic decomposition of fullerenes [23]. The coiled nanotubes were grown directly onto the HOPG substrate [23] and thus no manipulation of the sample was necessary for STM measurements. The tunneling parameters I_t and U_t were chosen in the same range as above.

3 Results and discussion

3.1 Irradiated multi-wall carbon nanotubes

STM investigations revealed that the nanotube defects created by irradiation appear as hillock-like features (Fig. 1b) with several angstroms in height, similar to the hillocks observed earlier on irradiated HOPG [24]. These hillocks could not be observed on the non-irradiated nanotubes (Fig. 1a). STS measurements (not presented here) show that the local electronic density of states (LDOS) near the Fermi level is higher at the defect sites than at the defect-free regions due to the presence of additional localized states [22]. The higher LDOS causes higher tunneling current at the defect sites which compels the STM

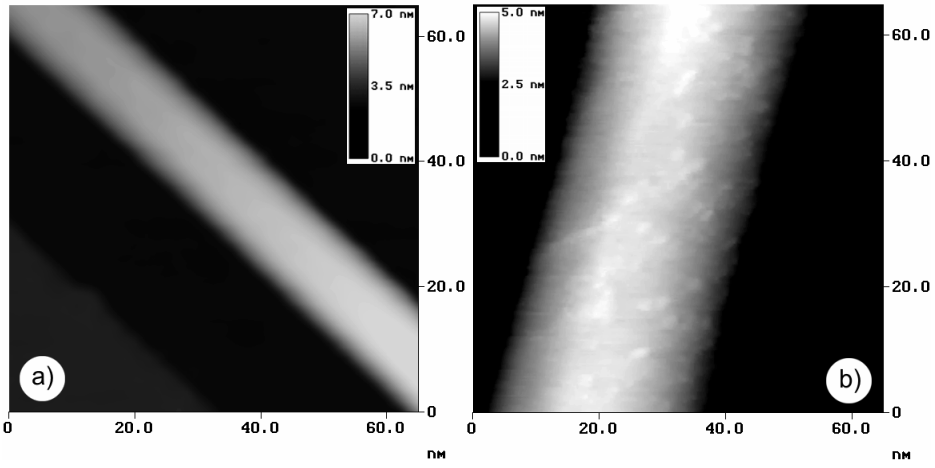

Fig. 1 STM images of multi-walled carbon nanotubes before (a) and after irradiation (b). The hillock-like features in (b) are the signatures of the irradiation induced defects.

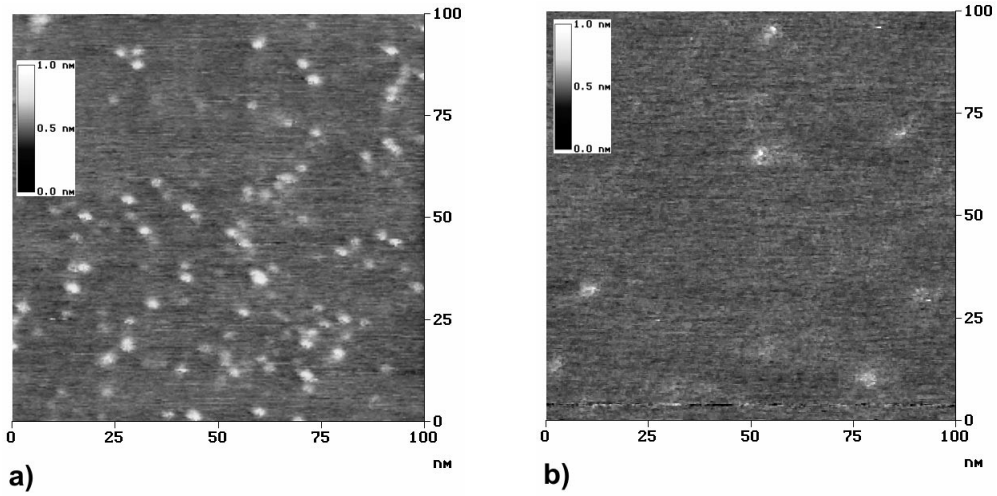

Fig. 2 Representative STM (a) and contact mode AFM images (b) of irradiated HOPG substrate.

tip to move upwards several angstroms in order to keep the tunneling current constant (the STM is operated in constant current mode). This vertical movement of the tip at the defect sites shows up as a hillock-like feature in the STM images [22]. This is in agreement with simulations, according to which vacancies appear as hillocks on the STM images [20].

In order to study further the origin of the observed hillocks, we performed both STM and contact mode AFM measurements on the irradiated HOPG substrate. In contact mode AFM the changes in the LDOS are not visible, only real topological surface variations are imaged. The measurements showed that 100–105 hillocks could be imaged on an area of 100×100 nm^2 by STM (Fig. 2a), while only 9–10 hillocks could be detected on a same size area by AFM (Fig. 2b).

These results show that the major part (~90%) of the hillock-like protrusions seen by STM is due to the change in the LDOS, and only a small part (~10%) can be attributed to clusters and deformations topographically emerging from the HOPG surface. Due to the graphitic structure of multi-walled nanotubes it is reasonable to assume a similar ratio for the hillocks observed on the nanotube surfaces.

The majority of the primary defects created by irradiation are vacancies, since at this ion energy the nuclear stopping dominates over the electronic stopping [25]. Air molecules adsorbed to these vacancies can also perturb the local electronic structure. Consequently, the height of the observed hillocks may be influenced by adsorbates. On the other hand, molecules adsorbed to vacancies do not induce significant topographic variations on the surface and thus these defects are less observed by AFM. Topographic deformations on the surface can for example appear when interstitial clusters form between the topmost graphitic layers [26, 27]. In this case the surface layer deforms and a hillock is produced right above the interstitial cluster, which can be detected by AFM. This hillock has a height similar to the one observed at vacancies [26].

3.2 Coiled carbon nanotubes

We observed hillock-like protrusions not only on the STM images of irradiated nanotubes but also during the STM investigation of as-grown coiled carbon nanotubes (Fig. 3b). Figure 3a shows a coiled nanotube synthesized by the decomposition of fullerenes [23], with 3.5 nm between the coils. Figure 3b shows a magnified portion from Fig. 3a), where one can observe the hillock-like features which appear repeatedly and regularly along the coils. The line-cuts in Fig. 4 show that the distances between the hillocks observed on the top of the coiled nanotube are in the range of 1.4–1.6 nm. According to theoretical models for coiled nanotube structures, pentagons and heptagons must be incorporated in a regular way in

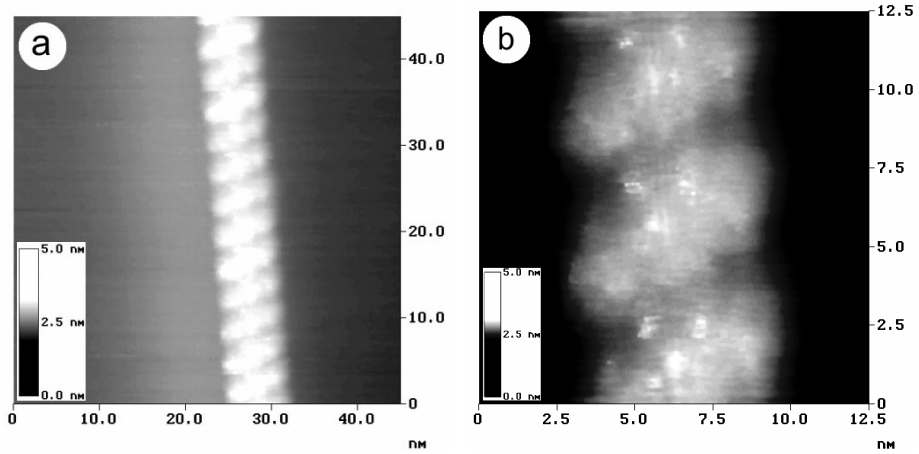

Fig. 3 STM images of a coiled carbon nanotube. The image in (b) shows a magnified portion from (a). The hillock-like features (bright spots) in (b) appear repeatedly and regularly along the coils. They are attributed to non-hexagonal carbon rings.

order to form stable coiling [9]. Pentagons induce positive curvature while heptagons induce a negative curvature in the hexagonal nanotube structure. It is also possible to build coiled nanotubes from azulene units where the non-hexagonal to hexagonal carbon ring ratio is close to unity [10]. In this case pentagons and heptagons are inserted regularly as well, although they are not considered defects any more, but ordinary building elements (haeckelite structure) [10]. The regular appearance of the hillocks along the coils in our measurements agrees well with the above model structures proposed for coiled nanotubes.

Furthermore, calculations show that pentagon and heptagon carbon rings incorporated in a hexagonal structure also change the LDOS by introducing additional electronic states near the Fermi level, and consequently they appear as hillocks on the STM images [18, 19]. Accordingly, we attribute the observed hillocks to the non-hexagonal carbon rings present in the structure, which are responsible for the bending and coiling of the nanotubes.

4 Conclusions

We presented experimental STM investigations of carbon nanotube point defects. The signatures of defects created by ion irradiation were studied and comparison was made with the signatures of regularly coiled carbon nanotube defects incorporated during growth. STM and AFM measurements on irradiated

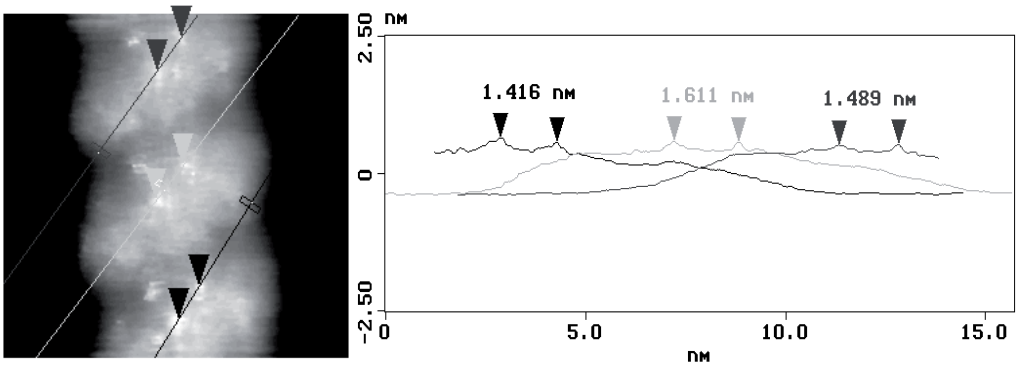

Fig. 4 Observed hillocks appear repeatedly and in a regular way along the coils. The line-cuts show the horizontal distance between the hillocks.

HOPG surface showed that the majority (~90%) of the defects (hillock-like protrusions) observed by STM is due to the change in the LDOS, and only a small part (~10%) can be attributed to clusters and deformations topographically emerging from the surface. We assume a similar ratio for the hillocks observed on the irradiated multi-wall nanotube surfaces.

Hillock-like protrusions were observed on the surface of as-grown coiled carbon nanotubes as well. The hillocks appeared repeatedly and regularly along the coils. These features were attributed to the non-hexagonal carbon rings incorporated during growth, which induce the coiling of the nanotubes. The regular appearance of the hillocks (non-hexagonal carbon rings) agrees well with earlier model structures proposed for coiled carbon nanotubes.

Acknowledgements This work has been done in the framework of the GDR-E No. 2756 (GDR on Science and Applications of Nanotubes – NANO-E). The authors acknowledge the financial support from OTKA Grant T43685 and NKTH grant MOFENACS in Hungary.

References

[1] J.-P. Salvetat, J.-M. Bonard, N. H. Thomson, A. J. Kulik, L. Forró, W. Benoit, and L. Zuppiroli, Appl. Phys. A **69**, 255 (1999).
[2] J. W. Park, J. Kim, J.-O. Lee, K. C. Kang, J.-J. Kim, and K.-H. Yoo, Appl. Phys. Lett. **80**, 133 (2002).
[3] M. T. Martínez, M. A. Callejas, A. M. Benito, M. Cochet, T. Seeger, A. Ansón, J. Schreiber, C. Gordon, C. Marhic, O. Chauvet, and W. K. Maser, Nanotechnology **14**, 691 (2003).
[4] F. Banhart, Rep. Prog. Phys. **62**, 1181 (1999).
[5] M. S. Raghuveer, P. G. Ganesan, J. D'Arcy-Gall, G. Ramanath, M. Marshall, and I. Petrov, Appl. Phys. Lett. **84**, 4484 (2004).
[6] V. Meunier, L. Henrard, and Ph. Lambin, Phys. Rev. B **57**, 2586 (1998).
[7] J. Han, M. P. Anantram, R. L. Jaffe, J. Kong, and H. Dai, Phys. Rev. B **57**, 14983 (1998).
[8] G. E. Scuseria, Chem. Phys. Lett. **195**, 534 (1992).
L. A. Chernozatonskii, Phys. Lett. A **172**, 173 (1992).
[9] S. Ihara, S. Itoh, and J. Kitakami, Phys. Rev. B **48**, 5643 (1993).
[10] L. P. Biró, G. I. Márk, A. A. Koós, J. B. Nagy, and Ph. Lambin, Phys. Rev. B **66**, 165405 (2002).
[11] M. Ishigami, H. J. Choi, S. Aloni, S. G. Louie, M. L. Cohen, and A. Zettl, Phys. Rev. Lett. **93**, 196803 (2004).
[12] H. Kim, J. Lee, S.-J. Kahng, Y.-W. Son, S. B. Lee, C.-K. Lee, J. Ihm, and Y. Kuk, Phys. Rev. Lett. **90**, 216107 (2003).
[13] P. Kim, T. W. Odom, J.-L. Huang, and C. M. Lieber, Phys. Rev. Lett. **82**, 1225 (1999).
[14] P. M. Ajayan, V. Ravikumar, and J.-C. Charlier, Phys. Rev. Lett. **81**, 1437 (1998).
[15] A. V. Krasheninnikov and K. Nordlund, Nucl. Instrum. Methods B **216**, 355 (2004).
[16] M. Terrones, F. Banhart, N. Grobert, J.-C. Charlier, H. Terrones, and P. M. Ajayan, Phys. Rev. Lett. **89**, 075505 (2002).
[17] A. Hashimoto, K. Suenaga, A. Glotter, K. Urita, and S. Iijina, Nature **430**, 870 (2004).
[18] V. Meunier and Ph. Lambin, Carbon **38**, 1729 (2000).
[19] D. Orlikowski, M. B. Nardelli, J. Bernholc, and C. Roland, Phys. Rev. B **61**, 14194 (2000).
[20] A. V. Krasheninnikov, K. Nordlund, M. Sirviö, E. Salonen, and J. Keinonen, Phys. Rev. B **63**, 245405 (2001).
[21] A. V. Krasheninnikov and K. Nordlund, Sov. Phys. Solid State **44**, 470 (2002).
[22] Z. Osváth, G. Vértesy, L. Tapasztó, F. Wéber, Z. E. Horváth, J. Gyulai, and L. P. Biró, Phys. Rev. B **72**, 045429 (2005).
[23] L. P. Biró, R. Ehlich, Z. Osváth, A. A. Koós, Z. E. Horváth, J. Gyulai, and J. B. Nagy, Mater. Sci. Eng. C **19**(3) (2002).
[24] L. Porte, M. Phaner, C. H. de Villeneuve, N. Moncoffre, and J. Tousset, Nucl. Instrum. Methods B **44**, 116 (1989).
[25] R. Spohr, in: Ion Tracks and Microtechnology: Principles and Applications, edited by Klaus Bethge (Friedr. Vieweg & Sohn Verlagsgesselschaft mbH, Braunschweig, 1990).
[26] J. R. Hahn and H. Kang, Phys. Rev. B **60**, 6007 (1999).
[27] V. F. Elesin and L. A. Openov, Surf. Sci. **442**, 131 (1999).

